Macromol. Symp. 2010, 296, 493–504 DOI: 10.1002/masy.201051066

Nanotopography Engineering on Homopolymeric Surfaces Using Cold Plasma Generated Charges

Sorin O. Manolache,[1] Klinsmann A. Gutierrez,[2] Charles D. Hall[2]*

Summary: Cold plasma as source for charged particles was used to induce nanotopographies on homopolymeric surfaces (nylon 12, PMMA, PMA, etc.). Hydrogen and helium plasmas were successfully used for surface nanoengineering of polymers using inductively coupled or atmospheric pressure non-equilibrium barrier discharge reactors. AFM analyses reveal the presence of nanotopographies on the treated surfaces. Physical factors control the process below the T_g and chemical factors dominate the process above T_g. Pyrolysis GC/MS analyses have been performed in order to obtain more information about the plasma processes. Cold plasma chemical processes, including charges effects are discussed as tools that open-up new ways for nanoengineering of the polymers' surfaces with specific functionalities and / or topography. Future nanomanufacturing techniques can generate anti-scratch, superhydrophobic or superhydrophilic properties on surface of every day use polymeric products by simple and convenient plasma enhanced processes.

Keywords: charges; cold plasma; homopolymers; nanotopography; Tg

Introduction

Miniaturization in the electronics industry,[1] the study of biomolecule immobilization and tissue engineering in biotech applications, MEMS transition to nanofabrication,[2] optoelectronic devices, conducting polymer/organic material devices, and materials with extreme properties (superhydrophilic, superhydrophobic, superoleophilic, etc.)[3–5] all require substrates with specific nanotopographies.

Many studies have demonstrated that nanotopographies (nano-grains, -pores, -particles, -ridges or -valleys) stimulate more possible responses from cells compared with conventional (nanosmooth) surface topographies[6]; however, the relative influence of nanotopography versus chemistry on cell response has not been well understand. Biotech applications have identified the importance of harmonization of nanotopography of substrate and the 3D shape of biomolecules (enzyme, proteins, RNA, DNA, etc.) or cells and tissues.[6–9] Investigations show that cells respond strongly to island-type nanotopography (cell types observed include endothelial cells, fibroblasts, osteoblasts, leukocytes and platelets); responses include differences in adhesion, growth, gene expression and morphology.[8–12] Extremely fine separation of DNA can be achieved using nanopatterned surfaces.[13]

Block copolymers[14–21] or mixtures of polymers[9,22] have been used as starting materials for the generation of nanopatterned and nanotopography controlled surfaces, to withstand environmental changes such as temperature, solvents, reactive chemical etching, absorption, etc. The nanotechniques for manufacturing nanopattern and nanotopography range from extremely simple ones such as rubbing

---

[1] Center for Plasma-Aided Manufacturing, University of Wisconsin - Madison, 1410 Engineering Drive #101, Madison WI 53706, USA
Fax: (608)262-3632;
E-mail: manolach@engr.wisc.edu

[2] Department of Electrical Engineering, University of Wisconsin - Madison, 1410 Engineering Drive #101, Madison WI 53706, USA

the substrate[23] or Langmuir-Blodgett films,[24] up to modified AFM (electrostatic nanolithography[25]) or TEM (carbothermal reduction)[26] analytical instrument operation. Self-assembling nanotechniques[27–30] are used to generate masks for selective processing of the surface (e.g., etching) or in the direct generation of nanotopography-containing substrates. Reactive chemical generation of nanotopography[31] and nanoparticle-induced nanopatterns[32] have also been used for bioapplications.

Various methods have been designed for nanotopography generation,[7–8] including extreme UV interference lithography (EUV-IL), soft-lithography techniques (e.g., replica molding (RM) and microcontact printing (μCP)), nanoimprint lithography (NIL), nanosphere lithography (NSL) (e.g., colloid lithography or block-copolymer micelle lithography), the nanostencil technique, direct-writing techniques (e-beam lithography (EBL)), focused ion-beam lithography (FIBL), dip-pen nanolithography (DPN), etc. However, these techniques are time consuming (i.e., requiring many steps), restricted to certain kind of materials,[14] and provide limited size/shape control of the nanostructures on the surface.

The use of large-scale production and/or cheap materials in new and more demanding fields or in the improvement of current state-of-the-art properties requires nanomanufacturing techniques that can modify the surface of the final objects. Superhydrophilic/superhydrophobic properties provide a good example: nanotopography must be present in order to get beyond the normal hydrophilicity range of the materials.[33–34] Investigations have been done in controlling surface roughness[35–36] at the nanoscale, chemical generation of nanopatterns using fatty-acids,[37] polyphosphazenes[38] or conducting polymers,[39] and nanotopography induced by nanoparticles.[40] Superhydrophobic cotton[41] and biomimetic nanosurfaces[42] have been reported. However, all the studied methods use *multi-step* processes and/or special composition layers and/or substrates.

Cold plasmas have been used as a step in nanotopographies / nanopatterns manufacturing,[15,43–46] especially in reactive ion etching of predeposited or self-assembled patterned masks into a surface.[1–2,27–30,47–48] Recent reports investigate the direct use of plasma for nanopatterning of silicone-based and nanocomposite materials,[49] for producing self-assembled layers of special polymers on surfaces,[47] and for directly producing micro- and nano-topography on PP, PET, PMMA, PTFE surfaces.[50–56] However, plasma literature reports changes, including those at the nanoscale, of the topography of treated or exposed substrates. The main hypothesis suggests material dependent selective etching of self-assembled nanodomains, thin film / macromolecules stretching, etc. Unfortunately, this excludes a possible solution for many commercially-available polymers. A systematic study is necessary to acquire basic knowledge about the mechanism in order to establish the theoretical and practical industrial tools in order to nanomanufacture surfaces without chemical restrictions related to their composition.

Previous findings from our research[57] indicate that cold plasma techniques may be used as a tool for nanoengineering of the polymer and inorganic surfaces with specific functionalities and topography. This paper present recent data showing the nanotopography effects of charges injected by plasma environment into polymeric surfaces in correlation to mobility of the macromolecular chains.

Experimental Part

Materials

Argon, helium and hydrogen supplied by Airgas Inc. (Radnor, PA), were used as the plasma gases for decontamination of the plasma reactor before experiments and as well as treatment gases. Nylon 12, poly (methyl methacrylate) (PMMA) and poly (methyl acrylate) (PMA) were purchased from Scientific Polymer Products, Inc. SP^2

(Omtario, NY) as pelettes or solution. Samples were spincoated onto 12 mm diameter stainless-steel mirror-polished discs from 3% w/w cresol (Nylon 12), dichloromethane (PMMA) and toluene (PMA) solutions; samples were heated at 60°C for 24 hours under vacuum for removal of the solvents. Sensors for etching / deposition monitor were also coated with thin polymeric layers by dipping into solutions, followed by drying for 24 hours under vacuum oven conditions.

Surface Plasma Treatment

Surface treatment of polymeric substrates was carried out by argon, helium or hydrogen plasma in a PlasmaTherm 790 Series Plasma Enhanced Chemical Vapor Deposition System (Oerlikon Corporate, Pfäfficon, Switzerland), an inductively coupled (25 cm diameter sample holder; ceramic walls, 30 cm internal diameter; mass flow and pressure controlled; computer controlled process with multiple steps) cylindrical reactor. The reactor is equipped with a 13.56 MHz radio frequency (RF2) and a 2 MHZ bias (RF1) power supplies. All the treatment parameters are monitored, controlled and logged by the computer software. Plasma experiments were preceded by a 10-min hydrogen plasma (400 W RF2, 200 W RF1, 10 mTorr) cleaning procedure to remove possible contaminants from earlier plasma reactions. In a typical experiment, after the substrates were placed on the sample holder, the reactor was evacuated to a base pressure level of 10^{-4}–10^{-5} Torr. RF2 was set to 200 W for all processes and only RF1 was varied for different biases applied to the polymeric surface; in this way the local heat on the surface of the sample was minimized. At the end of the process, the reactor was vented by filling with nitrogen and the samples were stored for further analysis.

Atmospheric pressure plasma modification of polymeric substrates has been done using a glass tubular reactor (inside diameter: 6 mm; outside diameter: 10 mm) with external ring copper electrodes (Figure 1) and powered at resonance (frequency: 26.3 kHz; voltage: 15 – 25 kV). Helium was used as plasma environment at a flow rate of 4 slm.

Metallic surfaces have been protected with dielectric (acrylic material) in order to reduce the loss of plasma generated charges to environment. Helium plasma flow has been directed to the polymeric surface of the sample.

Thickness Monitor

A STM – 100 / MF thickness monitor instrument (Sycon Instruments, Inc.; Syracuse, NY) have been used to monitor in real time the global changes of the polymeric layers. Polymeric layers were deposited by dipping the 6 MHz quartz crystals

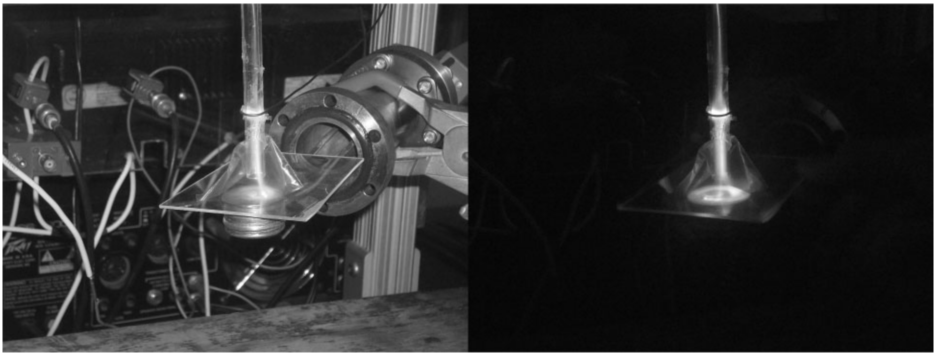

Figure 1.
Images of an atmospheric pressure non-equilibrium plasma reactor for treatment of thin polymeric films deposited on metalic substrates in ambient light (left) and dark conditions; helium flow rate: 4 slm; RF frequency: 26.3 kHz; voltage: 20 kV.

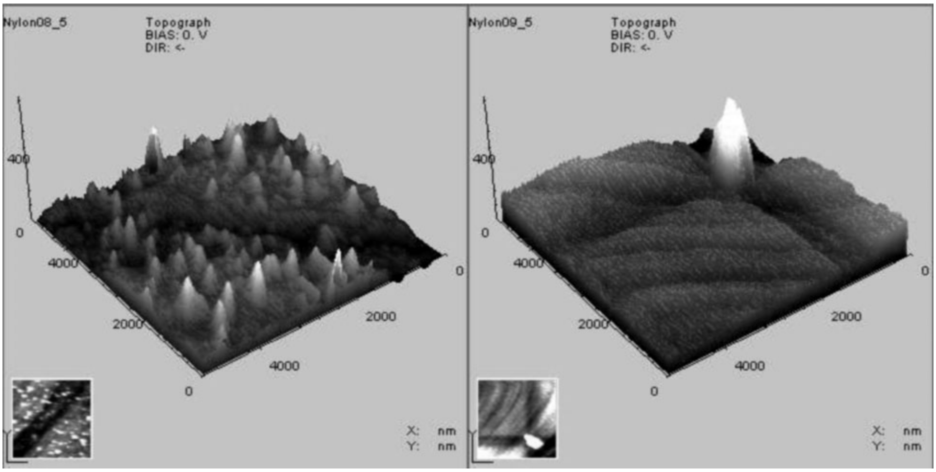

Figure 2.
AFM images of nylon 12 samples after hydrogen plasma treatment for 10 min; treatment temperature: 37°C; bias voltage: 180 V (left) and 100 V (right).

into of the polymer solution and evaporating the solvent under vacuum oven conditions for 24 hours. The polymeric layers were exposed to plasma environment in order to evaluate the global changes of the layers; thickness have been recorded using a LabView virtual instrument with a D/A card / PC system at 20 samples / s for at least 2 minutes; etching rates have been computed as slope of the recorded curves.

Topographical Analysis

Surface morphologies of unmodified and plasma treated surfaces were evaluated by atomic force microscopy (AFM) using a PicoScan instrument (Molecular Imaging, actual Agilent Technologies, Inc.) operated at 2 lines/s and 6 × 6 μm.

Chemical Analysis

Chemical structural information on untreated and plasma treated samples was obtained using pyrolysis GC/MS analysis. Nylon 12 or PMMA film was deposited on the pyrolyzer quartz tube from 5% solution in cresol or, respectively, dichloromethane. Both tubes and discs samples were treated in the plasma reactor using the selected parameters. The untreated and plasma treated coated tubes were pyrolyzed using a Pyroprobe 2000 equipment (CDS Analytical, Inc., Oxford, PA) at 400°C, 600°C, 800°C and 1000°C for 10 s and with the pyrolyzing chamber at 250°C. The gas products formed during the pyrolysis were identified and quantified using Gas Chromatography / Mass Spectrometry (GC-MS) technique (HP 5973 Mass Selective Detector and HP 6890 Series GC Systems by Agilent Technologies Co., formerly Hewlett-Packard Co.) employing the following experimental parameters: capillary column: HP-PLOT Q 30.0 m × 320.00 μm ID × 0.2 μm thick HP 19091P-Q04; carrier gas: chromatographic helium 99.9999% purity; constant flow: 2.3 ml/min; split inlet at 300°C; split ratio 10:1; oven at 30°C for 3 min, then 20°C/min to 110°C, 15°C/min to 170°C and 10°C/min to 260°C, final time: 30 min; post run heating at 260°C for 5 min; MSD transfer line heater temperature: 280°C; ionization chamber temperature: 230°C; quadrupole temperature: 150°C; MSD mode: scan; MSD recorded range: 10 – 600 amu; solvent delay time: 0.

Results and Discussion

Previous results[57] were indicating the bias voltage (the accelerating voltage for charged particles into surfaces exposed to plasma) as a main factor for generation of nanotopographies on homopolymeric surfaces exposed to electrical discharges. The bias voltage effects were modified by the macromolecular mobility (treatment temperature in respect to glass transition – Tg – of the polymer). However, the previous investigations were using various materials with different Tg plasma-modified at room temperature; the chemical composition of the material can change the chemistry of the plasma interaction with the exposed surfaces even on simple systems. Consequently, we selected for this study polymers with Tg close to room temperature (nylon 12: 37°C; PMA: 5°C) to be exposed to plasma interactions at various temperatures in respect to Tg.

A design of experiments (DoE) with Design Expert 7 (Stat-Easy Inc., Minneapolis, MN) was used to minimize the number of experiments; bias (20 – 180 V) and treatment temperature (17 - 57°C) were selected as parameters for hydrogen plasma treatment of nylon 12 (Tg 37°C). Hydrogen plasma produced by an inductively coupled installation was used as a source of charged particles that were accelerated by different bias voltages and injected into polymeric nylon 12 surfaces at various temperatures.

Figure 3 presents the nanotopographies generated after 10 min hydrogen plasma treatment at Tg; it can be noticed that extreme bias voltages (180 V) are produ-

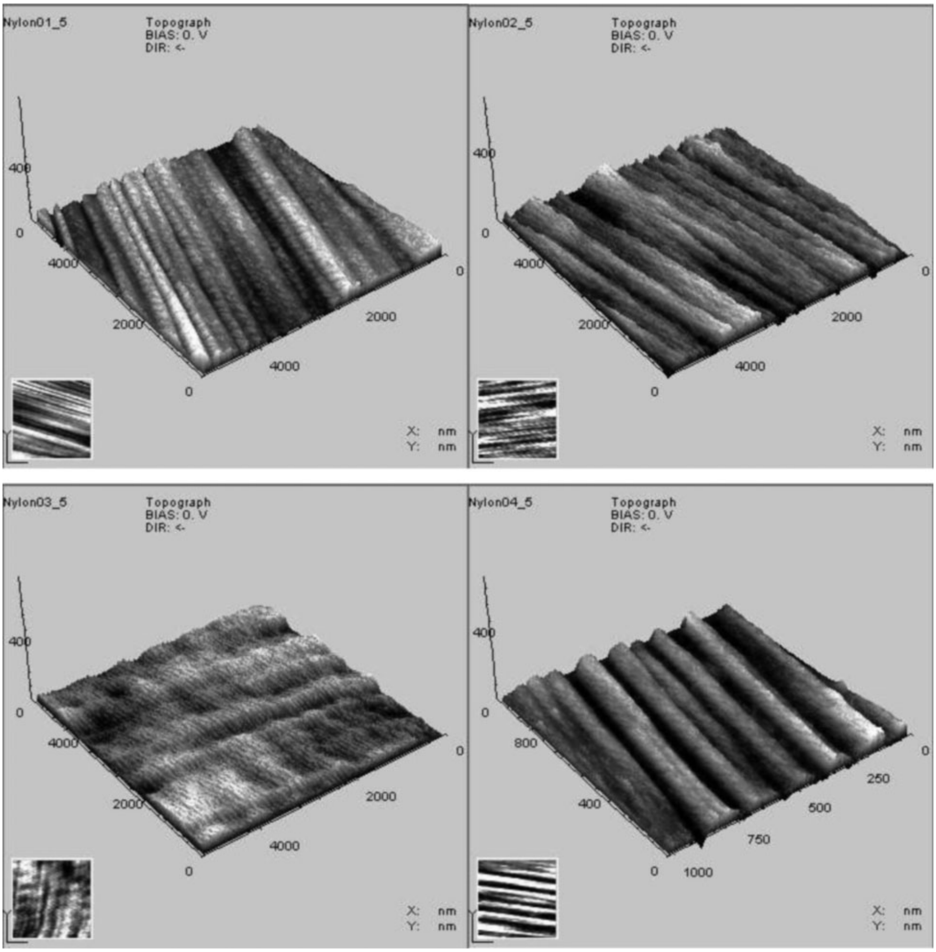

Figure 3.
AFM images of nylon 12 samples after hydrogen plasma treatment for 10 min; treatment temperature: 23°C (left) and 51°C (right); bias voltage: 45 V (top) and 157 V.

cing large conical-shape structures, while lower voltages (100 V) are generating extremely small features.

Nanotopographies generated on nylon 12 (Figure 3) at treatment temperature below Tg show small features (100 nm or smaller) developed on top of long range wavy surfaces (left side images). Treatments performed at temperature exceding Tg were producing only waving surfaces (wrinkles) at much larger scale (right side images) due to the increased mobility of the macromolecules exposed to plasma environment and charged particles.

Computation performed with CAChe software (Fujitsu Limited) show very small effects on molecule configurations exposed to electrical field comparable to the one created by the bias voltage used in these experiments. However, ions created on the molecular chains can produce dramatic changes in 3D-configuration under these environments.

Investigation of chemical modifications of nylon 12 after hydrogen plasma treatments have been performed using pyrolysis GC/MS techniques of films deposited on quartz tubes. Typical chromatograms and main chemical compounds are presented in Figure 4.

Quantitative analyses of the pyrolysis compounds at 800°C followed by GC/MS have been performed for propene, acetaldehyde, i-butene, butadiene, acetonitrile,

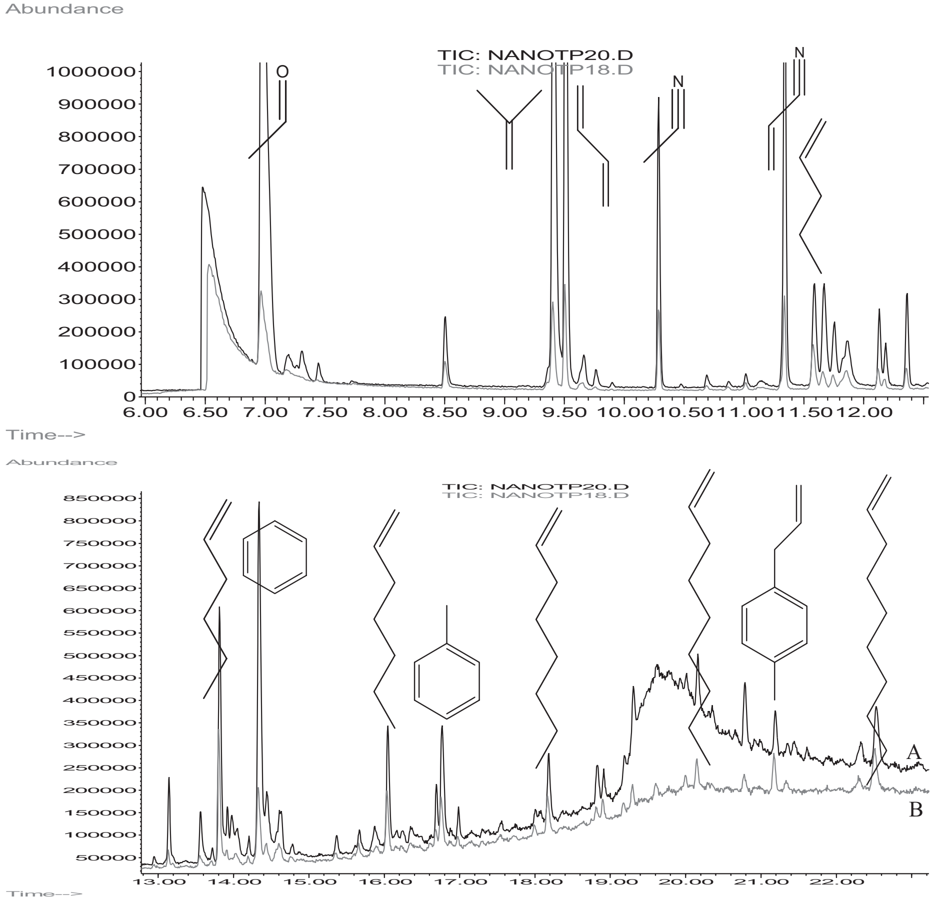

Figure 4.

Pyrolysis GC/MS chromatograms of hydrogen-plasma treated (A) and untreated (B) nylon 12 samples deposited on quartz tubes and the main chemical compounds.

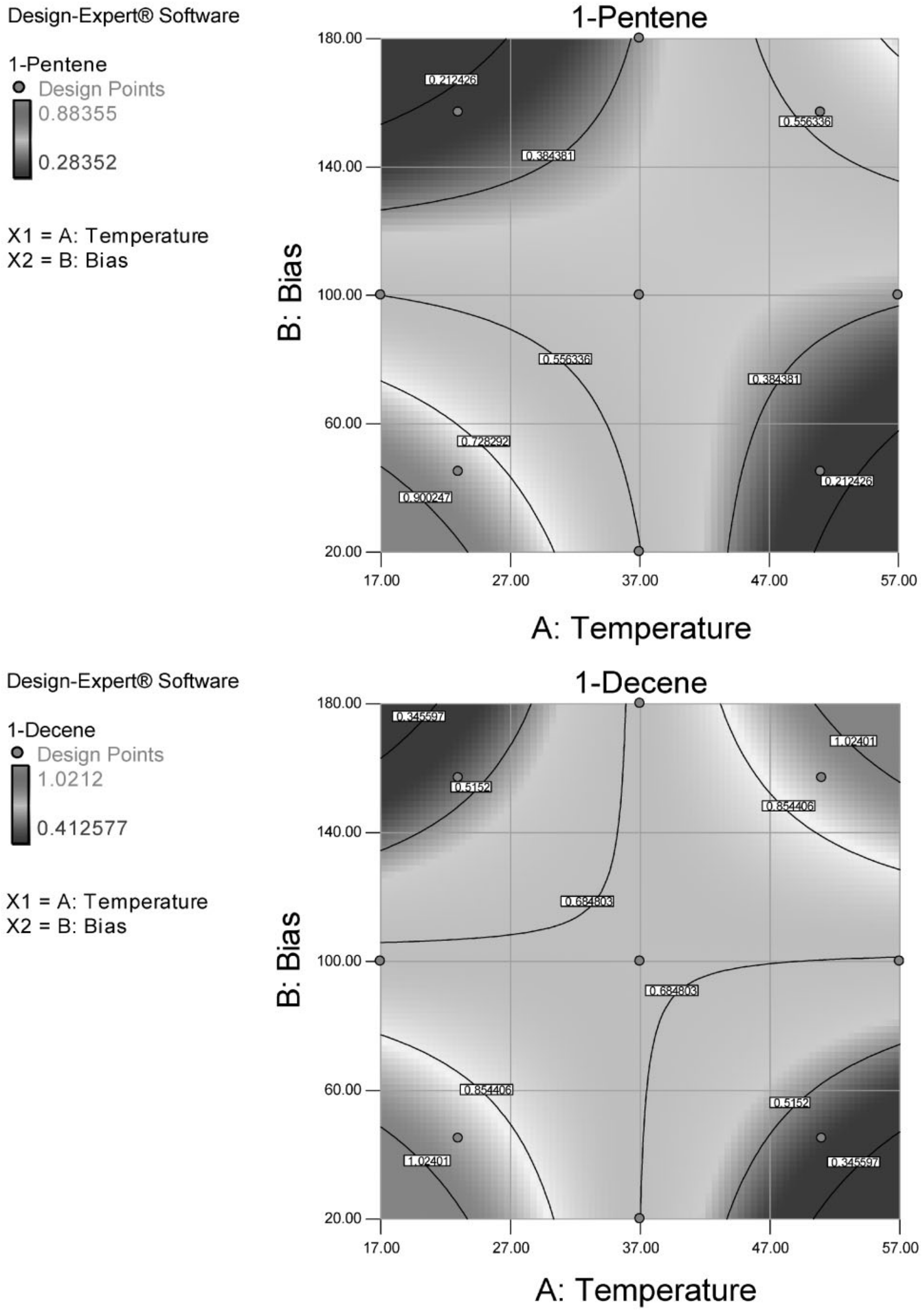

Figure 5.

The surface response of 1-pentene and 1-decene quantities (% v/v in total volatile compounds) generated by pyrolysis GC/MS.

3-propen-1-nitrile, 1-pentene, 1-hexene, benzen, 1-heptene, toluene, 1-octene, xylene, styrene, 1-nonene, benzonitrile, i-propenyl-benzen, 1-decene, etc. Fast thermal degradation (10 s at 800°C) of macromolecules is sensitive to the modifications produced in chemical structure; however, plasma environment affects only a thin surface layer[58–60] of the material that coexists with the unmodified bulk polymer. The quartz tubes have been coated with a very thin layer in order to minimize the contribution of bulk unmodified polymer in plasma treated samples.

Plasma experiments done on photoresists[58–60] (polymethacrylates) show an 1 – 2 nm modified layer on the surface enriched in carbon (amorphous diamond-like carbon – DLC) and an 100 nm layer where the fragmentation and/or crosslinking of the macromolecules dominate. The nanotopography changes and the stability of nanofeatures is affected by the mobility of the macromolecular chains; nylon 12 has long aliphatic flexible part that can be dramatically affected by crosslinking and chain fragmentation / degradation / branching.

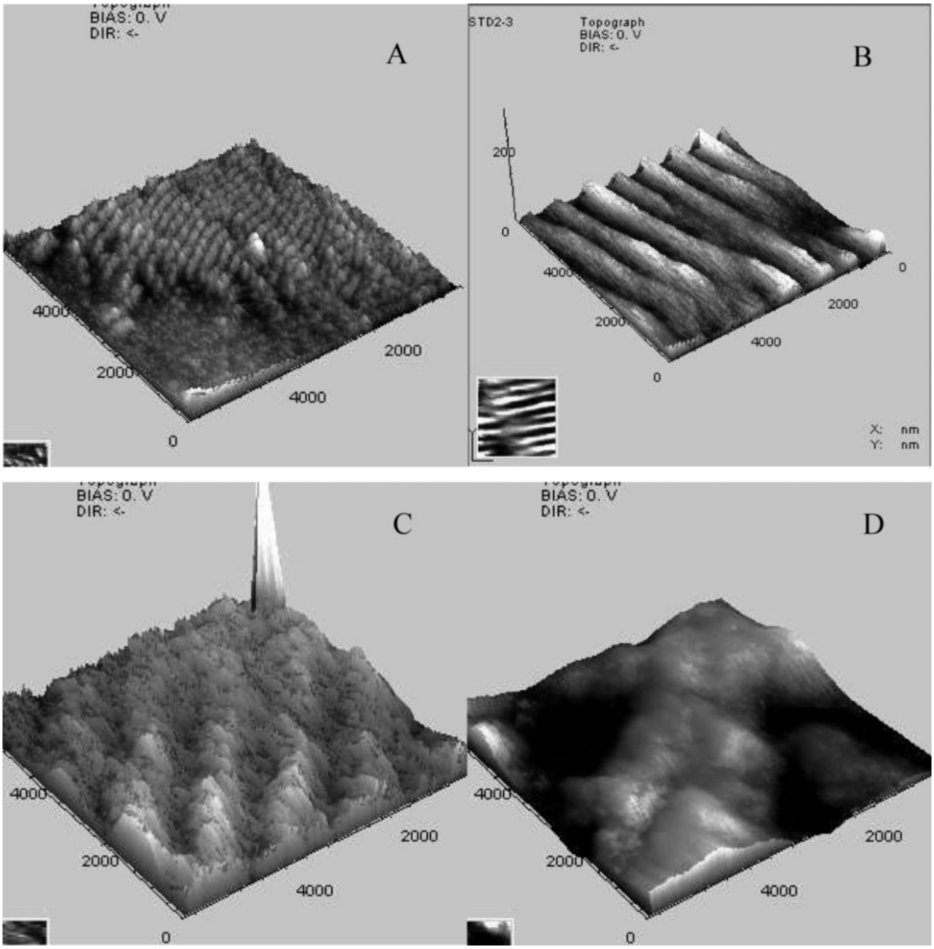

Figure 6.

AFM images of helium atmospheric pressure non-equilibrium plasma treated PMA samples; treatment conditions: A -9°C for 3 min; B 19°C for 3 min; C 5°C for 2 min; D 19°C for 9 min.

Plasma treatment produces free radicals that stabilize by cross-linking (high fluence of ions from plasma[58]) or macromolecular fragmentation / reattachment of small branches. As a result pyrolysis GC/MS show branched compounds and less linear alkenes during fast thermal degradation; the unmodified nylon 12 have better chance to produce alkenes (from 1-propene up to 1-decene; 1-undecene and 1-dodecene are missing due to decarbonylsation, nitriles and other compounds release from the ends of mers (Scheme 1)).

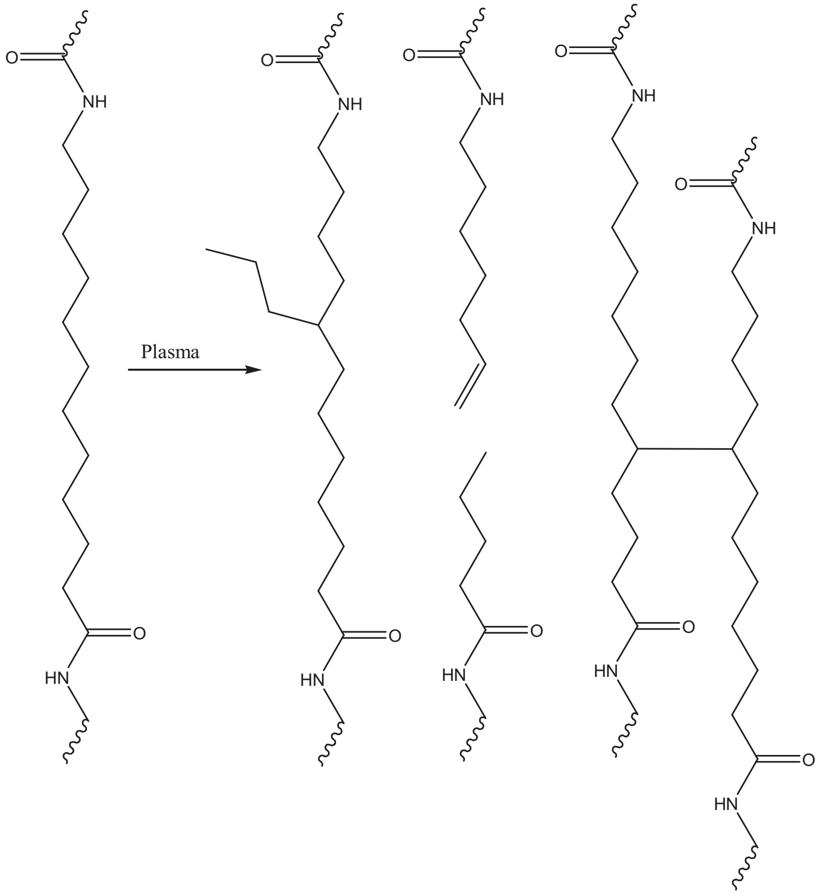

Scheme 1.

The regressions for 1-alkenes (contour diagrams in Figure 5 for 1-pentene and 1-decene) show domains at high bias voltage / low treatment temperature and low bias voltage / high treatment temperature (dark blue area) were the release of alkenes is decreased. However, the nanofeatures (Figures 2 and 3) are produced on surface of nylon 12 especially at high bias voltage / low treatment temperature; both the chemical compositions of polymer and plasma environment control the complex process of nanotopography modification.

The PMA (Tg: 5°C) represent also a good candidate to investigate the temperature influence near Tg for nanotopography generation after plasma treatment. Samples deposited on mirror-finished stainless-steel and having the temperature controlled by a 70 W thermoelectric device have been exposed to a helium atmospheric pressure non-equilibrium plasma. Figure 6 present typical nanotopographies generated by plasma exposure at various temperatures.

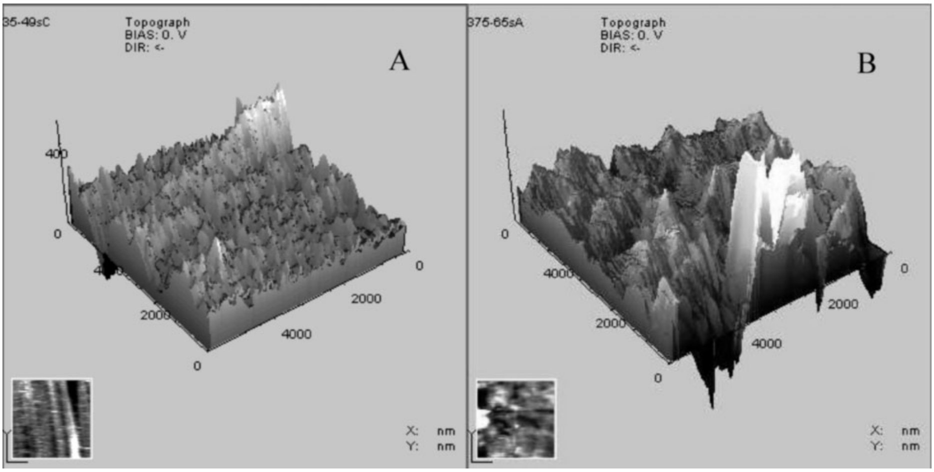

Figure 7.
AFM images of helium atmospheric pressure non-equilibrium plasma treated PMMA samples after 200 nm etching; A – 2 nm/s for 98 s; B – 3 nm/s for 65 s.

It can be noted similar waving surfaces (micron size wrinkles; Figure 6, B and D) generated during helium plasma exposure at temperature (19°C) higher than Tg. Lower treatment temperatures than Tg are producing nanofeatures smaller than 100 nm (Figure 6A) on the material surface. Treatments performed at Tg result in surfaces dominated by larger nanofeatures (over 100 nm) organized in micron size wrinkles (Figure 6 C).

Hypothesis such as selective etching of amorphous versus crystalline domains do not explain totally different nanotopographies generated on similar polymeric surfaces by different plasma environments. Etching / sputtering PMMA surfaces using a helium atmospheric pressure non equilibrium plasma have been performed at various etching rates. Figure 7 present topographies generated after 200 nm etching of the PMMA layer deposited on a quartz sensor for thickness monitoring and on a mirror finished stainless-steel. It can be noted totally different nanotopographies generated at different currents through the discharge (different charges transported from plasma environment to the walls, including the samples).

Conclusion

It has been shown that various nanotopographies can be successfully generated on the plasma-treated homogenous polymeric substrates. Charged particles delivered by plasma to exposed polymeric substrates are playing an important role for the nanotopography modification. Both chemical and physical factors are controlling the nanotopographies generated into polymers. Pyrolysis GC/MS data suggests that slight modifications of the polymers have been produced even on the environments with reduced chemical reactivity.

[1] Intel Co., http://software.intel.com/en-us/articles/2008-asia-academic-forum-keynotes/

[2] H. Luesebrink, T. Glinsner, S. C. Jakeway, H. J. Crabtree, N. S. Cameron, H. Roberge, T. Veres, *Journal of Nanoscience and Nanotechnology* **2005**, *5*(6), 864–868.

[3] E. Martines, K. Seunarine, H. Morgan, N. Gadegaard, C. D. W. Wilkinson, M. O. Riehle, *Nano Letters* **2005**, *5*(10), 2097–2103.

[4] J. Genzer, K. Efimenko, *Biofouling* **2006**, *22*(5), 339–360.

[5] S. Pilotek, H. Schmidt, *Hydrophobic and oleophobic coatings*, in: M. A., Aegerter, M. Mennig, Eds., Sol-Gel

Technologies for Glass Producers and Users, **2004**, 179–186

[6] M. Sato, T. J. Webster, *Nanomedicine* **2006**, *1*(3), 351–354.

[7] T. Blattler, C. Huwiler, M. Ochsner, B. Stadler, H. Solak, J. Voros, H. M. Grandin, *Journal of Nanoscience and Nanotechnology* **2006**, *6*(8), 2237–2264.

[8] A. Curtis, C. Wilkinson, *Trends in Biotechnology* **2001**, *19*(3), 97–101.

[9] M. J. Dalby, D. Pasqui, S. Affrossman, *IEE Proceedings: Nanobiotechnology* **2004**, *151*(2), 53–61.

[10] J. Yang, F. R. A. J. Rose, N. Gadegaard, M. R. Alexander, *Advanced Materials* **2009**, *21*(3), 300–304.

[11] C. Minelli, A. Kikuta, N. Tsud, M. D. Ball, A. Yamamoto, *Journal of Nanobiotechnology* **2008**, 6.

[12] L. R. Clements, Y.-L. Khung, H. Thissen, N. H. Voelcker, *Proceedings of SPIE* **2008**, *6799*, (BioMEMS and Nanotechnology III), 67990W/1-67990W/9.

[13] B. Li, X. Fang, H. Luo, Y.-S. Seo, E. Petersen, Y. Ji, M. Rafailovich, J. Sokolov, D. Gersappe, B. Chu, *Analytical Chemistry* **2006**, *78*(14), 4743–4751.

[14] K. Albrecht, A. Mourran, M. Moeller, *Advances in Polymer Science* **2006**, 200 (Ordered Polymeric Nanostructures at Surfaces), 57–70.

[15] G. E. Stein, E. J. Kramer, X. Li, J. Wang, *Polymer Preprints (American Chemical Society, Division of Polymer Chemistry)* **2006**, *47*(1), 525–526.

[16] H. Zhao, B. P. Farrell, D. A. Shipp, *Polymer* **2004**, *45*(13), 4473–4481.

[17] Y. Chen, H. Huang, Z. Hu, He. Ti, *Langmuir* **2004**, *20*(9), 3805–3808.

[18] A. W. Harant, C. N. Bowman, *Polymer Preprints (ACS, Division of Polymer Chemistry)* **2003**, *44*(2), 204–205.

[19] J. P. Spatz, P. Eibeck, S. Moessmer, M. Moeller, E. Y. Kramarenko, P. G. Khalatur, I. I. Potemkin, A. R. Khokhlov, R. G. Winkler, P. Reineker, *Macromolecules* **2000**, *33*(1), 150–157.

[20] I. I. Potemkin, E. Y. Kramarenko, A. R. Khokhlov, R. G. Winkler, P. Reineker, P. Eibeck, J. P. Spatz, M. Moeller, *Langmuir* **1999**, *15*(21), 7290–7298.

[21] M. Moeller, J. P. Spatz, S. Moessmer, P. Eibeck, P. Ziemann, B. Kabius, *Polymeric Materials Science and Engineering* **1999**, *80*, 3–4.

[22] S. Santer, A. Kopyshev, H.-K. Yang, J. Ruehe, *Macromolecules* **2006**, *39*(8), 3056–3064.

[23] T. Blattler, C. Huwiler, M. Ochsner, B. Stadler, H. Solak, J. Voros, H. M. Grandin, *Journal of Nanoscience and Nanotechnology* **2006**, *6*(8), 2237–2264.

[24] S. Dai, X. Zhang, Z. Du, H. Dang, *Materials Letters* **2004**, *59*(4), 423–429.

[25] S. Jegadesan, S. Sindhu, S. Valiyaveettil, *Small* **2006**, *2*(4), 481–484.

[26] P. Arumugam, S. S. Shinozaki, R. Wang, G. Mao, S. L. Brock, *Chemical Communications (Cambridge, United Kingdom)* **2006**, *10*, 1121–1123.

[27] Y. Mori, R. Saito, *Kagaku (Kyoto, Japan)* **2003**, *58*(7), 66–67.

[28] B. K. Yoon, W. Hwang, Y. J. Park, J. Hwang, C. Park, J. Chang, *Macromolecular Research* **2005**, *13*(5), 435–440.

[29] D. Falconnet, D. Pasqui, S. Park, R. Eckert, H. Schift, J. Gobrecht, R. Barbucci, M. Textor, *Nano Letters* **2004**, *4*(10), 1909–1914 .

[30] S.-H. Lee, F. S. Diana, A. Badolato, P. M. Petroff, E. J. Kramer, *Journal of Applied Physics* **2004**, *95*(10), 5922–5924.

[31] K. L. Christman, M. V. Requa, V. E. Enriquez-Rios, S. C. Ward, K. A. Bradley, K. L. Turner, H. D. Maynard, *PMSE Preprints* **2006**, *94*, 31.

[32] K. Ishizu, T. Kojima, Y. Ohta, T. Shibuya, *Journal of Colloid and Interface Science* **2004**, *272*(1), 76–81.

[33] E. Martines, K. Seunarine, H. Morgan, N. Gadegaard, C. D. W. Wilkinson, M. O. Riehle, *Nano Letters* **2005**, *5*(10), 2097–2103.

[34] A. R. Phani, V. Grossi, M. Passacantando, S. Santucci, *Journal of Experimental Nanoscience* **2007**, *2*(1 & 2), 63–71.

[35] N. Michael, B. Bhushan, *Microelectronic Engineering* **2007**, *84*(3), 382–386.

[36] H. J. Lee, S. Michielsen, *Journal of Polymer Science, Part B: Polymer Physics* **2006**, *45*(3), 253–261.

[37] S. Wang, Y. Song, L. Jiang, *Nanotechnology* **2007**, *18*(1), 015103/1–015103/5.

[38] H. R. Allcock, L. B. Steely, A. Singh, *Polymer International* **2006**, *55*(6), 621–625.

[39] M. Woodson, J. Liu, *Journal of the American Chemical Society* **2006**, *128*(11), 3760–3763.

[40] M. Yu, G. Gu, W.-D. Meng, F.-L. Qing, *Applied Surface Science* **2007**, *253*(7), 3669–3673.

[41] Y. Inoue, N. Saito, O. Takai, *Hyomen Gijutsu* **2005**, *56*(7), 379–384.

[42] K. Ostrikov, H.-J. Yoon, A. E. Rider, S. V. Vladimirov, *Plasma Processes and Polymers* **2007**, *4*(1), 27–40.

[43] E. Sardella, P. Favia, R. Gristina, M. Nardulli, R. d'Agostino, *Plasma Processes and Polymers* **2006**, *3*(6/7), 456–469.

[44] A. Valsesia, P. Colpo, T. Meziani, F. Bretagnol, M. Lejeune, F. Rossi, A. Bouma, M. Garcia-Parajo, *Advanced Functional Materials* **2006**, *16*(9), 1242–1246.

[45] S. Kiyohara, H. Takamatsu, T. Motoishi, K. Mori, *Materials Research Society Symposium Proceedings* **2004**, EXS-2 (Nontraditional Approaches to Patterning), 73–75.

[46] P. Visconti, C. Turco, R. Rinaldi, R. Cingolani, *Microelectronic Engineering* **2000**, *53*(1–4), 391–394.

[47] D.-G. Choi, H. K. Yu, S. G. Jang, S.-M. Yang, *Journal of the American Chemical Society* **2004**, *126*(22), 7019–7025.

[48] D.-G. Choi, S. G. Jang, H. K. Yu, S.-M. Yang, *Chemistry of Materials* **2004**, *16*(18), 3410–3413.

[49] R. Job, Y. L. Huang, Y. Ma, B. Zoelgert, W. Duengen, *Materials Research Society Symposium*

Proceedings **2005**, *849*, (Kinetics-Driven Nanopatterning on Surfaces), 103–108.

[50] C. C. Martine, R. Lehmann, P. Groening, L. Schlapbach, *Applied Surface Science* **2003**, *207*(1–4), 276–286.

[51] J. Yang, F. R. A. J. Rose, N. Gadegaard, M. R. Alexander, *Langmuir* **2009**, *25*(5), 2567–2571.

[52] A. Ruiz, A. Valsesia, G. Ceccone, D. Gilliland, P. Colpo, F. Rossi, *Langmuir* **2007**, *23*(26), 12984–12989.

[53] K. Tsougeni, A. Tserepi, G. Boulousis, V. Constantoudis, E. Gogolides, *Japanese Journal of Applied Physics, Part 1: Regular Papers, Brief Communications & Review Papers* **2007**, *46*(2), 744–750.

[54] A. Tserepi, E. Gogolides, K. Tsougeni, V. Constantoudis, E. S. Valamontes, *Journal of Applied Physics* **2005**, *98*(11), 113502/1–113502/6.

[55] E.-S. Yoon, S. H. Yang, H. Kong, K.-H. Kim, *Tribology Letters* **2003**, *15*(2), 145–154.

[56] C. Borcia, G. Borcia, N. Dumitrascu, *Journal of Optoelectronics and Advanced Materials* **2008**, *10*(3), 675–679.

[57] S. Manolache, H. Jiang, F. S. Denes, *Polymer Surface Modifications: Relevance to adhesion* **2009**, *5*, 45–62.

[58] E. Pargon, D. Nest, D. B. Graves, *Journal of Vacuum Science & Technology, B: Microelectronics and Nanometer Structures–Processing, Measurement, and Phenomena* **2007**, *25*(4), 1236–1243.

[59] D. Nest, D. B. Graves, S. Engelmann, R. L. Bruce, F. Weilnboeck, G. S. Oehrlein, C. Andes, E. A. Hudson, *Applied Physics Letters* **2008**, *92*(15), 153113/1–153113/3.

[60] M. J. Titus, D. G. Nest, T.-Y. Chung, D. B. Graves, *Journal of Physics D: Applied Physics* **2009**, *42*(24) 245205/1–245205/13.